

AN INTERNATIONAL EFFORT TO COMPARE GAS HYDRATE RESERVOIR SIMULATORS

Joseph W. Wilder¹, George J. Moridis², Scott J. Wilson³, Masanori Kurihara⁴, Mark D. White⁵, Yoshihiro Masuda⁶, Brian J. Anderson^{7,8*}, Timothy S. Collett⁹, Robert B. Hunter¹⁰, Hideo Narita¹¹, Mehran Pooladi-Darvish¹², Kelly Rose⁷, Ray Boswell⁷

¹Department of Theoretical & Applied Math
University of Akron
302 Buchtel Common
Akron, OH 44325-4002 USA

⁷National Energy Technology Laboratory
3610 Collins Ferry Road
P.O. Box 880
Morgantown, WV 26507 USA

²Lawrence Berkeley National Laboratory,
University of California
Earth Sciences Division, 1 Cyclotron Rd., MS
90-1116
Berkeley, CA 94720 USA

⁸West Virginia University
Department of Chemical Engineering
Morgantown, WV 26506-6102 USA

³Ryder Scott Company, Petroleum
Consultants
621 17th Street, Suite 1550
Denver, Colorado 80293 USA

⁹US Geological Survey
Denver Federal Center, MS-939
Box 25046
Denver, CO 80225 USA

⁴Japan Oil Engineering Company, Ltd.
Kachidoki Sun-Square
1-7-3, Kachidoki, Chuo-ku,
Tokyo 104-0054, Japan

¹⁰ ASRC Energy Services
3900 C Street, Suite 702,
Anchorage, AK 99503 USA

⁵ Pacific Northwest National Laboratory
Hydrology Group
PO Box 999
Richland, WA 99352 USA

¹¹National Institute of Advanced Industrial
Science and Technology
Methane Hydrate Research Laboratory
2-17-2-1, Tsukisamu-Higashi
Toyohiraku, Sapporo, Hokkaido 062-8517
Japan

⁶Department of Geosystem Engineering
University of Tokyo Japan

¹²Fekete Associates Inc.
Suite 2000, 540-5th Avenue S.W.
Calgary, Alberta T2P 0M2 Canada

ABSTRACT

This collaborative effort to compare the world's leading gas hydrate reservoir simulators is designed primarily to exchange information and insight that will lead to the improvement in simulation capability of experimental and naturally occurring gas hydrate accumulations. The initial phase of the code comparison activity achieved the simulation of five problems of increasing complexity by five different reservoir simulators: CMG STARS, HydrateResSim, MH-21 HYDRES, STOMP-HYD, and TOUGH+HYDRATE. The cases run, the results obtained, and an analysis of those results is available to the gas hydrates community through the DOE/NETL website[1].

Results of the Problem 1 (non-isothermal multi-fluid transition to equilibrium (no hydrate); and Problem 2 (closed-domain gas hydrate dissociation) indicated very close agreement among the simulators. This agreement suggests that all had consistently captured the basics of mass and heat transfer, as well as overall process of gas hydrate dissociation. Problem 3 (dissociation in a one-

dimensional domain), which included several scenarios, one in which ice formation was likely, produced the initial divergence among the simulators. Other differences were noted in both Problem 4 (gas hydrate dissociation in a one-dimensional radial domain) and Problem 5 (gas hydrate dissociation in a two-dimensional radial domain), resulting in significant corrections to algorithms within several of the simulators. Given the lack of real world data for validation purposes, these improvements would likely not have been identified without the comparison activity. This paper will outline the nature of the first five cases studies of the code comparison effort and their results.

Keywords: gas hydrates; reservoir simulations; production modeling; porous media

NOMENCLATURE

P	pressure [MPa]
Q_H	heat flux [Watts]
Q	fluid flux [kg/s]
r	radial dimension [meters]
r_w	outer radial dimension of a well [meters]
t	time [seconds]
T	temperature [K or °C]
β_{gl}	interfacial tension scaling factor
h_{gl}	gas-aqueous capillary pressure head [meters]
k_{rG}	gas-phase relative permeability
k_{rA}	aqueous-phase relative permeability
\bar{S}_A	effective aqueous saturation
S_A	aqueous saturation
S_G	gas saturation
S_H	hydrate saturation
S_{irA}	irreducible aqueous saturation

INTRODUCTION

This collaborative, international effort to compare gas hydrate reservoir simulators is designed to: (1) to exchange information regarding gas hydrate dissociation and physical properties enabling improvements in reservoir modeling, (2) to build confidence in all the leading simulators through exchange of ideas and cross-validation of simulator results on common datasets of escalating complexity, and (3) to establish a depository of gas hydrate related experiment/production scenarios with the associated predictions of these established simulators that can be used for ongoing and future comparison purposes.

In the first part of this effort, five problems have been developed for comparison purposes and simulated by five different reservoir simulators, CMG STARS [2], HydrateResSim [3], MH-21 HYDRES [4], STOMP-HYD [5], and

TOUGH+HYDRATE [6]. The five problems range in complexity from one-dimensional to three-dimensional (with radial symmetry), and in horizontal dimensions of 20 meters to 1 kilometer. Each of the problems and the results of the comparisons to date are described below.

PROBLEM 1

Base Case (Non-isothermal Multi-fluid Transition to Equilibrium)

Processes of interest to the simulation of CH₄ production from gas hydrates in porous media include multfluid flow and heat transport along with complex phase transitions, including hydrate dissociation and formation. Before executing problems with the additional complexities involved with the gas hydrate phase, a base case problem was designed to examine the numerical simulation of multfluid flow and heat transport processes with a single phase transition from aqueous saturated to unsaturated conditions for a water-CH₄ system outside the stability region for gas hydrate formation. The problem involved a horizontal one-dimensional closed domain (no flow boundary conditions), initialized with gradients in aqueous pressure, gas pressure, and temperature that yield aqueous saturated conditions on half of the domain and aqueous unsaturated conditions on the other half of the domain. The simulation then proceeded to an equilibrium condition in pressure and temperature. The results of numerical simulations of CH₄ hydrate formations in geologic media largely depend on the computation of thermodynamic and transport properties. Therefore, a portion of this problem involves reporting property data for selected temperatures and pressures.

Base Case Problem Description

Gradients in aqueous pressure, gas pressure, and temperature are imposed across a 20-m one-

dimensional horizontal domain, discretized using uniformly spaced 1-m grid cells. A horizontal domain is used to eliminate gravitational body forces from the problem, as an additional simplification. The pressure and temperature gradients are specified to yield aqueous saturation conditions in the first 10 grid cells and aqueous unsaturated conditions in the remaining 10 grid cells. The simulation then proceeds to equilibrium conditions in pressure, phase saturations, and temperature. The list of processes simulated in this problem include:

1. aqueous-gas multifluid flow subject to relative permeability, capillary effects, and phase transition from aqueous saturated to unsaturated
2. heat transport across multifluid porous media with phase advection and component diffusion
3. change in CH₄ solubility in water with pressure and temperature
4. change in thermodynamic and transport properties with pressure and temperature

The van Genuchten capillary pressure model was used to express the relationship between gas aqueous capillary pressure head and the aqueous saturation [7]:

$$\bar{S}_A = \frac{S_A - S_{irA}}{1 - S_{irA}} = \left[1 + (\alpha \beta_{gl} h_{gl})^n \right]^{-m}; \quad (1)$$

$$\text{where } m = 1 - \frac{1}{n}$$

The Mualem [8] porosity distribution function, when combined with the van Genuchten capillary pressure relationship yields the following functions for aqueous and gas phase relative permeability:

$$k_{rA} = (\bar{S}_A)^{1/2} \left[1 - \left(1 - (\bar{S}_A)^{1/m} \right)^m \right]^2 \quad (2)$$

$$k_{rG} = (1 - \bar{S}_A)^{1/2} \left[\left(1 - (\bar{S}_A)^{1/m} \right)^m \right]^2 \quad (3)$$

Simulation Results

Profiles of temperature, aqueous saturation, dissolved CH₄ mass fraction and aqueous pressure at selected times (i.e., 0, 1, 10, 100, 1,000, and 10,000 days) were calculated using all 5 different simulation packages and sample results for the aqueous saturation are shown in Figure 1.

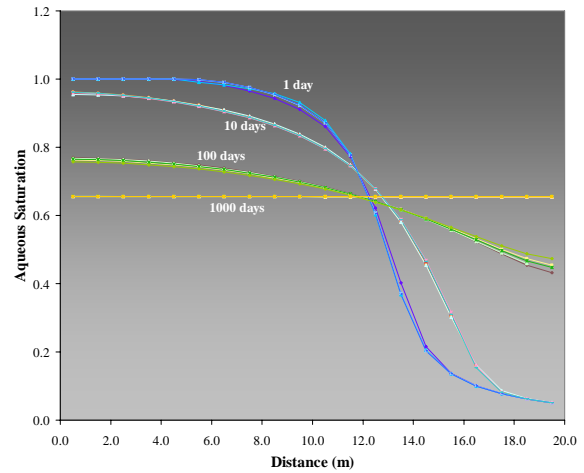


Figure 1: Aqueous saturation for 1, 10, 100, and 1000 days as calculated by the code comparison participants

The calculated profiles show that, for the total system, equilibrium conditions are achieved by 10,000 days. Aqueous pressure and saturation reach equilibrium conditions by 1,000 days indicating the faster response of the hydrologic system compared against the thermal system; where the temperature does not reach equilibrium conditions until 10,000 days. Transition to thermal equilibrium progresses rapidly until the hydrologic system reaches equilibrium by 1,000 days. From here, progress toward thermal equilibrium is dependent on low gradients and diffusive heat transfer. Likewise, transition to equilibrium for the dissolved CH₄ proceeds rapidly until 1,000 days, where advances toward equilibrium are controlled by aqueous and gas diffusion processes.

PROBLEM 2

Base Case with Gas Hydrate (Closed-Domain Hydrate Dissociation)

This second problem uses the same closed horizontal domain as in Problem 1, but includes gas hydrate in the half of the spatial domain that only contained water in Problem 1. The initial conditions are such that for long times (i.e. time > 1,000 days) the system approaches an equilibrium state in which all of the hydrate has dissociated via the thermal energy available in the half of the spatial domain initially containing only gas and water. From the specified initial conditions, the simulation proceeds to an equilibrium temperature and pressure state resulting from the complete dissociation of the gas hydrate initially present in the reservoir. Again, there was excellent

agreement among the five simulators tested in terms of the rates of movement of the gas hydrate front as well as the predicted phase saturations.

Problem Description

One half ($x < 10$ m) of a 20-m, one-dimensional horizontal domain, discretized using uniformly spaced 1.0 m and 0.1 m grid cells was initialized with aqueous-hydrate conditions ($S_H = 0.4$); whereas, the other half of the domain is initialized with gas-aqueous conditions ($S_G = 0.539474$). As with the Base Case problem (Problem 1), a closed horizontal domain is used to eliminate gravitational body forces and boundary condition effects. The initial conditions are specified to yield complete dissociation of the hydrate, via the thermal capacitance of the domain-half initialized with gas-aqueous conditions. To initialize the aqueous-hydrate half of the domain, temperature, pressure, and hydrate saturation were specified. For reference purposes, hydrate equilibrium pressure, hydration number, and cage occupancies were also specified for this half of the domain. To initialize the gas aqueous half of the domain temperature, aqueous pressure and gas pressure were specified.

All active phases (i.e., aqueous, gas, and hydrate) were assumed to comprise water and CH_4 , and capillarity was assumed between the active phases. Hydrate dissociation was assumed to occur using equilibrium kinetics (i.e., infinitely fast dissociation rates). The simulations proceeded to equilibrium conditions in temperature and pressure, dissociating the hydrate during the transition process and leaving gas-aqueous conditions.

The list of processes simulated in this problem include:

1. multifluid flow for an aqueous-gas-hydrate system in geological media, subject to relative permeability and capillarity effects and phase transitions
2. dissociation of CH_4 hydrate in response to thermal stimulation and depressurization
3. heat transport across multifluid geological media with phase advection and component diffusion
4. change in CH_4 solubility in water with pressure and temperature
5. change in thermodynamic and transport properties with pressure and temperature

Simulation Results

Profiles of temperature, aqueous saturation, hydrate saturation, gas saturation, aqueous pressure, and CH_4 mass fractions in the active phases at selected times (0, 1, 10, 100, 1,000, and 10,000 days) were calculated and compared among the simulators. Hydrate dissociation occurred initially in response to both thermal stimulation and depressurization; however, later in time dissociation is principally due to thermal stimulation as the released CH_4 gas increases the system pressure above the initial conditions. Initially hydrate dissociation occurs without hydrate creation. After 10 days, however, hydrate dissociation occurs in conjunction with hydrate creation on the hydrate-side of the dissociation front (Figure 2). Hydrate creation is caused by the released CH_4 gas migrating into the hydrate-side of the domain forming new hydrate. This hydrate eventually dissociates as the dissociation front proceeds toward the hydrate side ($x < 10$ m) of the domain.

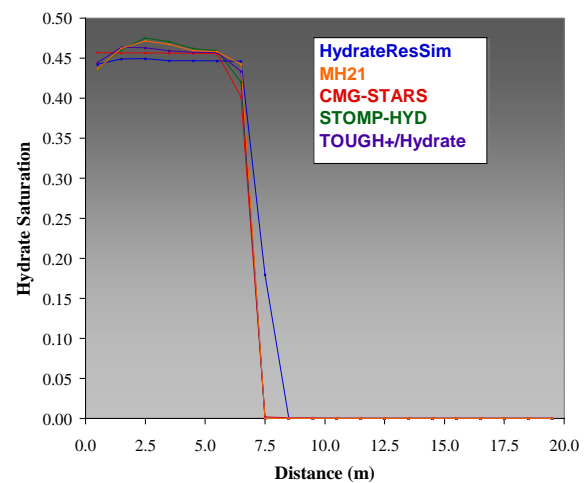


Figure 2: Hydrate saturation at 100 days as calculated by the code comparison participants for Problem 2

As was seen in Problem 1, the five simulators exhibited similar results, both qualitatively and quantitatively. Shown in Figure 3 is a plot of the gas saturation as a function of horizontal distance for this 1-dimensional system. As can be seen, subtle differences between some of the simulators are becoming evident, particularly among gas and aqueous saturations. As expected due to the development history, TOUGH+Hydrate [6] and HydrateResSim [3] show very similar results with only slight differences. STOMP-HYD, MH-21,

and CMG-STARS results show a more gradual decrease in gas saturation on the hydrate side of the dissociation front, seemingly indicating slower movement of the gas away from the hydrate.

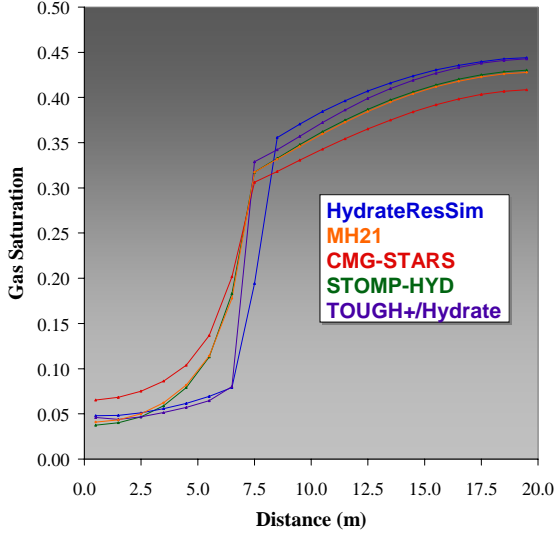


Figure 3: Gas saturation at 100 days as calculated by the code comparison participants for Problem 2

PROBLEM 3

Dissociation in a 1-D Open Domain

The third problem again involves a one-dimension spatial domain. While Problem 2 explored the behavior of the simulators when gas hydrate dissociated in the (larger) closed domain of Problem 1, the intent of Problem 3 is to explore fine-scale effects of gas hydrate dissociation in a system open to gas release from the origin. To explore the range of potential behavior, three separate cases were defined and compared: (1) dissociation due to thermal stimulation, (2) dissociation due to depressurization to a pressure above the quadruple point (ensuring that no ice forms in the reservoir), and (3) dissociation to a pressure below the quadruple point (allowing the formation of ice).

Problem Description

The domain modeled in Problem 3 is a one-dimensional Cartesian system with $L \times W \times H = 1.5 \text{ m} \times 1.0 \text{ m} \times 1.0 \text{ m}$ and a discretization of $30 \times 1 \times 1$ uniformly-sized gridblocks in x , y , and z . The initial pressure of the domain was 8 MPa and the initial temperature was 2°C for the thermal stimulation case (1) and 6°C for the two depressurization cases (2 and 3). The initial

saturations for all three cases were $S_H = 0.5$, $S_A = 0.5$, $S_G = 0.0$. The Stone [9] + Aziz [10] relative permeability model was used in Problem 3:

$$k_{rG} = (\bar{S}_G)^n, \quad \bar{S}_G = \frac{(S_G - S_{irG})}{(1 - S_{irA})} \quad (4)$$

$$k_{rA} = (\bar{S}_A)^n, \quad \bar{S}_A = \frac{(S_A - S_{irA})}{(1 - S_{irA})} \quad (5)$$

For this problem, $n = 3.0$, $S_{irA} = 0.12$, and $S_{irG} = 0.02$.

Boundary Conditions

The boundary conditions were specified for three different cases, each leading to different hydrate dissociation scenarios.

For all cases:

At $x = X_{max}$: No mass or heat flow

At $x = 0$: Constant $S_A = 1.0$

Case 1: *Thermal stimulation*

Constant $P_0 = P_i$

Constant $T(x = 0) = 45^\circ\text{C}$

Case 2: *Depressurization to a pressure above the Q -point, no ice formation*

Constant $T_0 = T_i = 6^\circ\text{C}$

Constant $P(x = 0) = 2.8 \text{ MPa}$

Case 3: *Depressurization to a pressure below the Q -point, leading to ice formation*

Constant $T_0 = T_i = 6^\circ\text{C}$

Constant $P(x = 0) = 0.5 \text{ MPa}$

Simulation Results

While good agreement was generally observed among the simulators for the first two cases (see Figures 4 and 5), the third case (which resulted in the formation of ice in some portions of the reservoir) revealed differences in the location of the hydrate dissociation front over time (see Figure 6). The observed differences most likely are the result of the different manners in which the appearance and effects of ice are modeled in the various simulators. One should note the relative time-dependent decrease in hydrate saturation near the origin (wellbore). For Case 1, as shown in Figure 4, the hydrate dissociation front has moved approximately 0.5 m for all simulators over the course of 3 days, while for Case 2 (Figure 5) the front has moved about 0.4 m in the same timeframe. Case 3 (Figure 6) shows the fastest

movement of the dissociation front, 0.3 to 0.5 m in 20 minutes; however, for simulations with longer radial dimensions it is expected to see significant detrimental effects on gas rate from hydrate production due to ice formation.

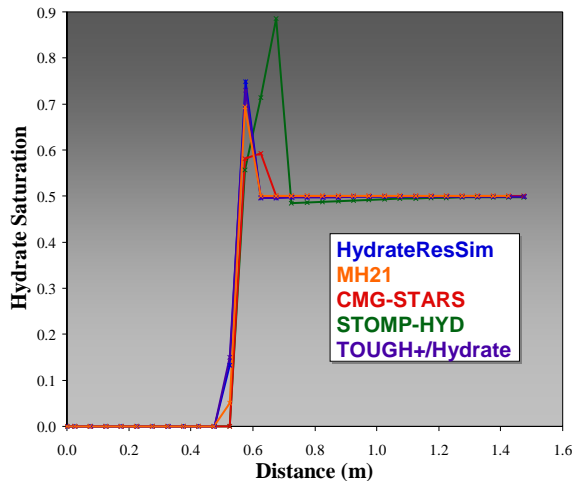


Figure 4: Hydrate saturation after 3 days as calculated by the code comparison participants for the thermal stimulation case above the quadruple point (case 1) of Problem 3.

PROBLEM 4
Gas Hydrate Dissociation in a One-dimensional Radial Domain – Similarity Solutions

The fourth problem models gas hydrate dissociation in a one-dimensional radial domain. The fine discretization utilized in this problem is needed to accurately capture the simulated front during thermal dissociation. As with Problem 3, this problem explores the fine scale effects of hydrate disassociation in a non-closed system. This problem was designed to take advantage of the fact that under proper conditions, hydrate dissociation results in solutions that are of the form of “similarity solutions.”

These solutions are ones in which the observed values of any variable (e.g., temperature, pressure, saturation, etc.) depend only on the ratio r^2/t (where r is the radial distance from the well and t is time). This implies that if one plots results from different times on a single plot using r^2/t as the independent variable, all of the curves should lie on top of each other (except for small variations due to transient behavior at small values of t).

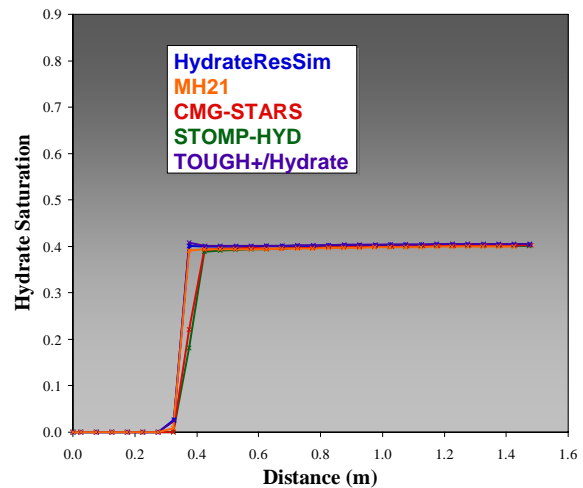


Figure 5: Hydrate saturation after 3 days as calculated by the code comparison participants for the depressurization case above the quadruple point (case 2) of Problem 3.

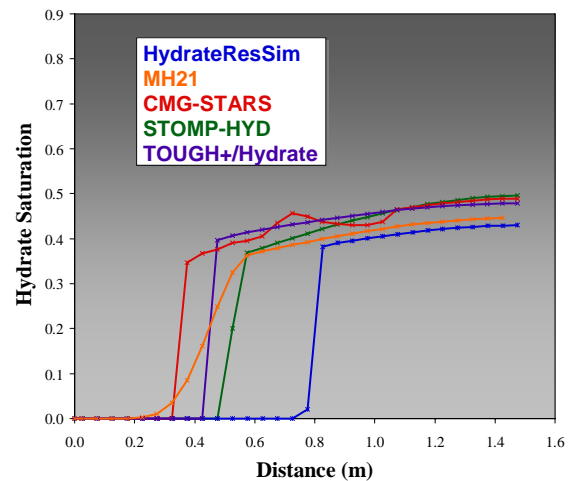


Figure 6: Hydrate saturation after 20 minutes as calculated by the code comparison participants for the depressurization case below the quadruple point (case 3) of Problem 3.

Problem Description

The domain modeled in Problem 4 is a one-dimensional radial system with $L \times H = 1000 \text{ m} \times 1.0 \text{ m}$ and a discretization of 1000 uniform 0.02-m gridblocks from $r = 0.0 \text{ m}$ to $r = 20 \text{ m}$ and 1000 gridblocks logarithmically distributed from $r = 20 \text{ m}$ to $r = 1000 \text{ m}$. The Stone [9] + Aziz [10] relative permeability model (Equations (4) and (5)) was again used in Problem 4 with the same parameters as were used in Problem 3.

Initial Conditions

Case 1: $P_i = 4.6$ MPa, $T_i = 3^\circ\text{C}$, $S_H = 0.5$, $S_A = 0.5$
Thermal stimulation

Case 2: $P_i = 9.5$ MPa, $T_i = 12^\circ\text{C}$, $S_H = 0.4$, $S_A = 0.6$
Depressurization

Boundary Conditions

The boundary conditions were specified for two different cases.

For both cases:

At $r = R_{max}$: Constant pressure, temperature, and saturations

Case 1: Thermal stimulation

At $r = 0$: $Q_H = 150$ W

Case 2: Depressurization

At $r = 0$: $Q = 0.1$ kg/s including gas and aqueous phase

Simulation Results

This problem represents the closest to a problem with a “known” solution for hydrate systems. The observation that the tested simulators (HydrateResSim, MH-21, TOUGH+HYDRATE, STOMP-HYD, and HydrateResSim) showed the same similarity solution-type behavior (see Figure 7) is an indication that they all are capturing the same physical process which leads to this behavior.

For the thermal dissociation problem, heat is added at the well at a rate of 150 W. The saturation distributions in Figure 7 indicate a very sharp dissociation front. For this particular problem, the front occurs near $r^2/t = 0.04$ m²/day. Thus, at $t = 20$ days, the dissociation front will be at a radius of

$$r = (0.04 \text{ m}^2/\text{day} \times 20 \text{ days})^{1/2} = 0.89 \text{ m}$$

Similarly, at $t = 100$ days, the dissociation front will be at a radius of

$$r = (0.04 \times 100)^{1/2} = 2.0 \text{ m.}$$

A very interesting observation is that thermal dissociation creates a self-sharpening front, which develops as the higher pressure of the released gas leads to the formation of additional hydrates immediately ahead of the dissociation front ($r \approx 0.2$ m). This is clearly demonstrated by the step in front of the sharp dissociation front in the hydrate saturation in Figure 7.

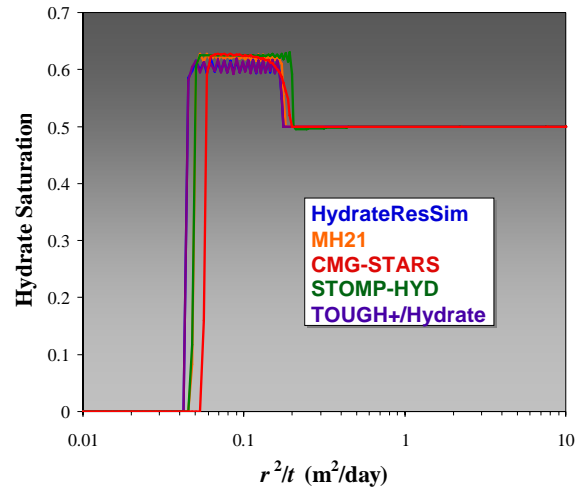


Figure 7: Plot of r^2/t for the five different simulators for Case 1 (thermal stimulation) at $t = 10$ days.

For the case of depressurization, fluids are removed through the well at a rate of $Q = 0.1$ kg/s. The results shown in Figure 8 illustrate that the curves are invariant, and confirm that the radial hydrate depressurization problem in one-dimension has a similarity solution. The saturation distributions in Figure 8 indicate that the dissociation front is not as sharp as in the case of thermal stimulation, but more diffuse. Actually, it can be argued that a dissociation zone (rather than the front) is the result of this depressurization-induced dissociation, and the onset of this dissociation zone is very well defined, between 0.02 and 0.04 m for all five simulators.

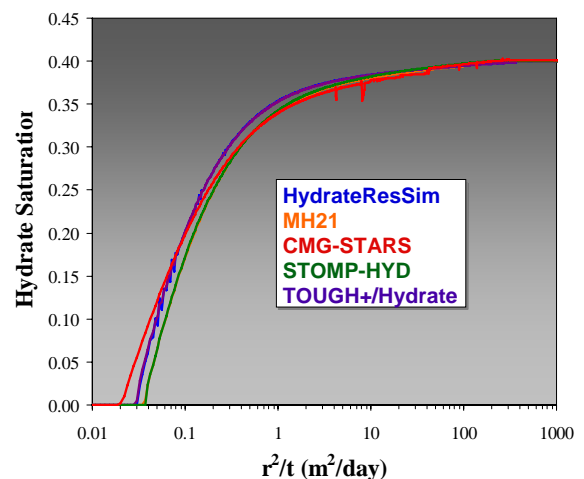


Figure 8: Plot of r^2/t for the five different simulators for Case 2 (depressurization) at $t = 10$ days.

For this particular problem, the onset of the dissociation zone occurs near $r^2/t = 0.03 \text{ m}^2/\text{day}$, and the zone (defined as the region in which the gas saturation is non-zero) extends to $r^2/t \approx 200 \text{ m}^2/\text{day}$. Thus, at $t = 20$ days, the dissociation front will be at a radius of

$$r = (0.03 \times 20)^{1/2} = 0.77 \text{ m},$$

and the dissociation zone will extend from 0.77 m to

$$r = (200 \times 20)^{1/2} = 63 \text{ m}$$

Similarly, at $t = 100$ days, the dissociation front will be at a radius of

$$r = (0.03 \times 100)^{1/2} = 1.7 \text{ m},$$

and the dissociation zone will extend from 1.7 m to

$$r = (200 \times 100)^{1/2} = 140 \text{ m}$$

These results indicate the substantial efficiency advantage of depressurization as a method of gas production from hydrate dissociation under these simulated conditions. As discussed in our companion paper, the initial temperature of a reservoir strongly affects gas production rates from depressurization [11].

Implications of the Similarity Analysis

1. If the problem has similarity solutions, the distributions of any of the variables describing the problem (e.g., pressure, temperature, phase saturation, etc.) are invariant when plotted against r^2/t . For example, if one plots hydrate saturation vs. r^2/t at any time t , all the curves will coincide.
2. If the problem has similarity solutions, there is no need to conduct simulations over the entire time frame. The results at any time are sufficient to describe system behavior and performance at any time.
3. The similarity solution can provide a simple and robust tool to evaluate the production potential of hydrate deposits. To accomplish this, one can develop simple graphical solutions for very complex problems by obtaining a family of similarity graphs for different conditions (as a function of initial saturation, heat input, etc.). Once this is done, there is no need for numerical simulation.
4. Because we showed that this 1-D hydrate problem has a similarity solution, any numerical solution must be invariant when plotted against r^2/t . This is a robust tool for the evaluation of the accuracy of any numerical simulator of hydrate behavior. If the simulator

is inaccurate, then the solutions at different times will not coincide.

This similarity solution to the hydrate problem is based on a one-dimensional radial problem. In natural systems, vertical temperature and pressure gradients, as well as reservoir heterogeneity will likely cause difficulty in finding a similarity solution.

PROBLEM 5

Gas Hydrate Dissociation in a Two-dimensional Radial Domain

The fifth problem models gas hydrate dissociation in a two-dimensional radial domain. In this problem, a 10 meter-thick gas hydrate-bearing sandstone is bounded vertically by two 25 meter-thick shales, as illustrated in Figure 9. The length and height of the domain are 1000 meters by 60 meters with four different discretization models. Problem 5 seeks to investigate a range of behavior by simulating two separate cases: (Case A) 80% initial methane hydrate saturation, and (Case B) 70% initial methane hydrate saturation.

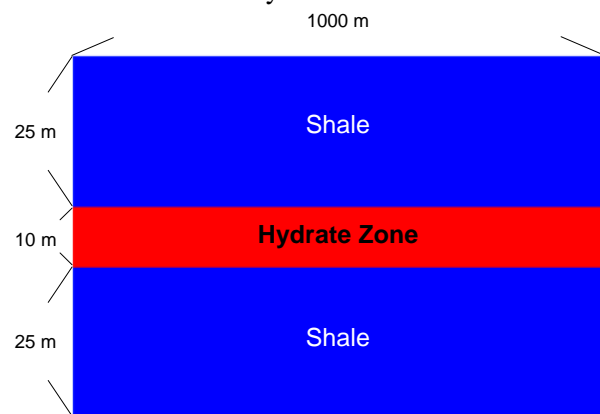


Figure 9: Schematic of the hydrate and boundary domains for Problem 5.

Problem Setup

In addition to examining the effect of initial hydrate saturation on gas hydrate production, we examined the effect of gridding. Four different discretization scenarios were implemented for both of the two cases in Problem 5:

Model 1 (200 x 30)

r direction : 200 cells logarithmically distributed from $r_w = 0.10795 \text{ m}$ to $r_{200} = 1000 \text{ m}$

z direction : 30 cells (5 x 5 m, 20 x 0.5 m, 5 x 5 m)

Model 2 (200 x 11)

r direction : 200 cells logarithmically distributed from $r_w = 0.10795$ m to $r_{200} = 1000$ m

z direction : 11 cells (5 x 5 m, 1 x 10.0 m, 5 x 5 m)

Model 3 (50 x 30)

r direction : 50 cells logarithmically distributed from $r_w = 0.10795$ m to $r_{50} = 1000$ m

z direction : 30 cells (5 x 5 m, 20 x 0.5 m, 5 x 5 m)

Model 4 (50 x 11)

r direction : 50 cells logarithmically distributed from $r_w = 0.10795$ m to $r_{50} = 1000$ m

z direction : 11 cells (5 x 5 m, 1 x 10.0 m, 5 x 5 m)

The Stone [9] + Aziz [10] relative permeability model (Equations (4) and (5)) was again used in Problem 5, with $n = 3$ and the irreducible saturations given in Table 1. These irreducible water saturations, paired with the initial hydrate saturations for Cases A and B result in initial free water saturations of 5% and 10% for Case A and B respectively.

Table 1: Irreducible saturations for the relative permeability functions in Problem 5

Case	S_{wir} (%)	S_{Gir} (%)
Case A	15	2
Case B	20	2

Simulation Results

As suggested in Figure 12, when the methane hydrate zone is divided into 20 grid blocks with thickness of 0.5 m, it can be predicted that the methane hydrate located nearer to the upper and lower shale zones are dissociated preferentially, due to heat supply from these shale zones. Once the methane hydrate at the locations adjacent to the shale zones is dissociated, the permeability is drastically improved at these locations and the low bottomhole flowing pressure can be transferred to more distant areas from the wellbore, which results in the significant increase in the gas production rate as shown in Figures 10 and 13. The gas production rates predicted with Model 1 (200 x 30) are approximately 5 times larger than those predicted with Model 2 (200 x 11) for both Case A and Case B.

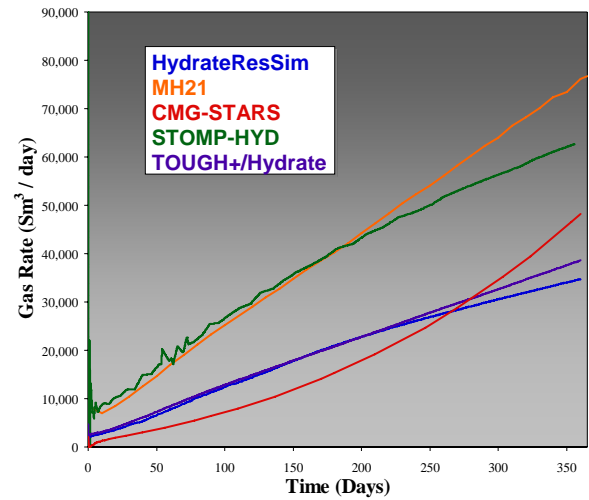


Figure 10: Predicted gas rate for Problem 5, Case A Model 1 (5A-1).

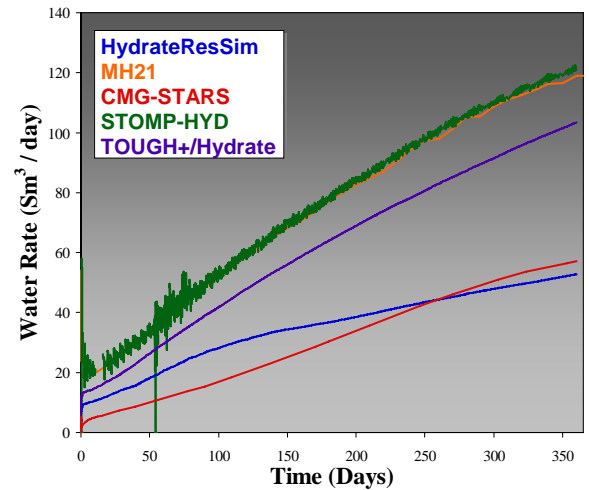


Figure 11: Predicted water rate for Problem 5, Case A Model 1 (5A-1).

Examining the differences between the gas rates as predicted for Case A and Case B illustrates the importance of the initial free water saturation of the reservoir. For identical discretizations (Model 1) Case B (Figures 14 and 15) results in a gas and water production rate nearly twice that found in Case A (Figures 10 and 11) for all simulators. This rate increase can be directly attributed to the free pore water that results in higher aqueous relative permeabilities allowing the faster movement of fluids and the relatively rapid transmission of the pressure front away from the hydrate dissociation front.

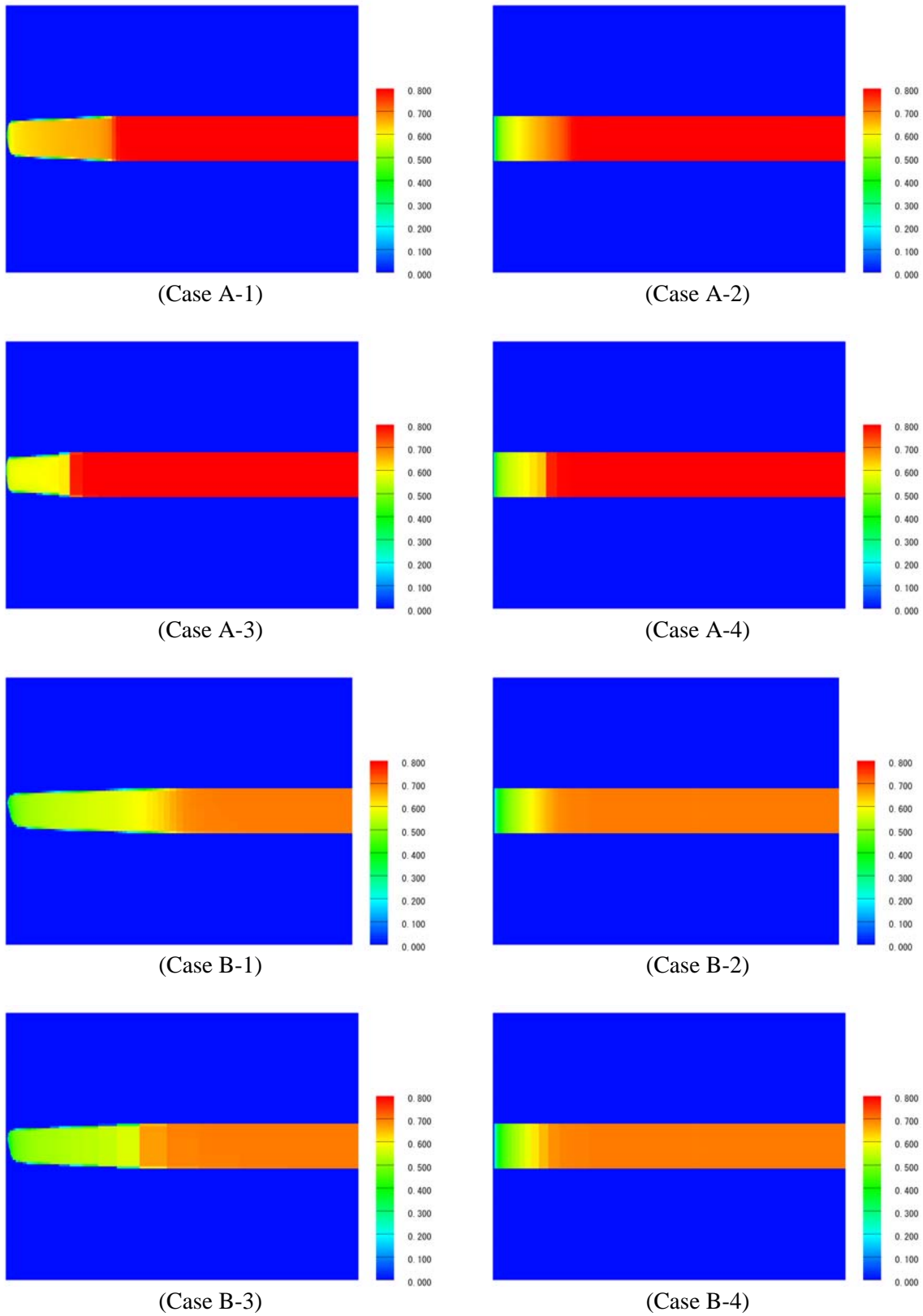


Figure 12: Methane Hydrate Saturation Distribution as simulated by MH-21 (after 270 days, fraction).

Therefore, the characterization of free pore water is of the utmost importance for the prediction of gas production from a hydrate accumulation. In a companion paper [11] we present the results of a history-matching exercise to Modular Dynamics Test (MDT) results. The importance of the free pore water on gas production from hydrate deposits is reemphasized in the results from long-term production modeling based on those history-matched parameters.

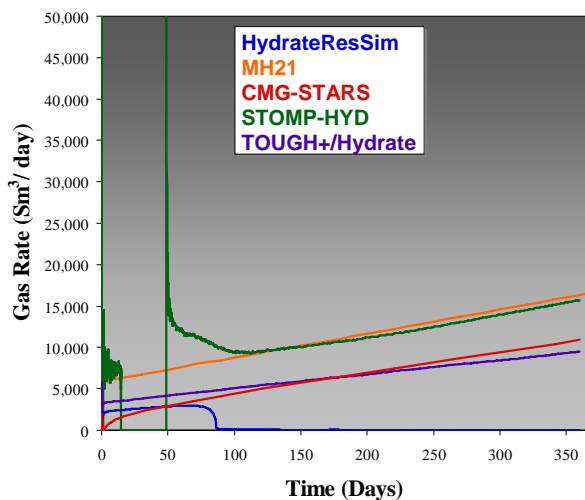


Figure 13: Predicted gas rate for Problem 5, Case A Model 2 (5A-2).

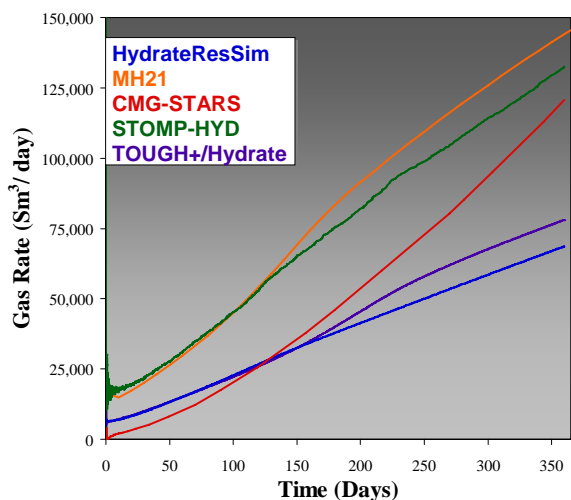


Figure 14: Predicted gas rate for Problem 5, Case B Model 1 (5B-1).

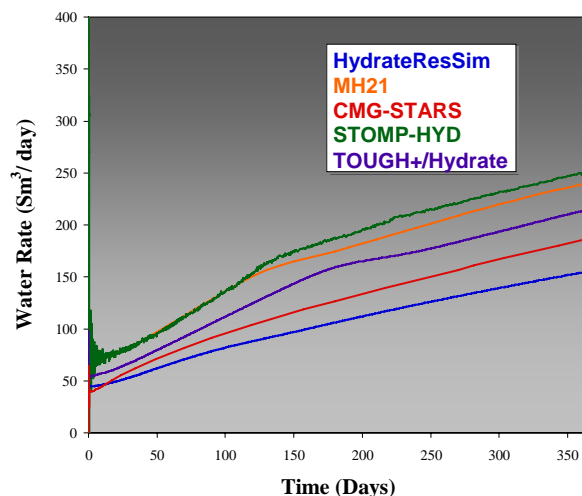


Figure 15: Predicted water rate for Problem 5, Case B Model 1 (5B-1).

CONCLUSIONS

Simulation of gas hydrate reservoir production involves the solution of a complex combination of highly coupled fluid, heat, and mass transport equations combined with the potential for formation and/or disappearance of multiple solid phases in the system. Also, the physical and chemical properties of the geologic media containing gas hydrate are highly dependent on the amount of gas hydrate present in the system at any given time. Gas hydrate modelers have used many different conceptual models and mathematical algorithms to solve these problems; each approach has certain advantages and disadvantages but none is either completely accurate or proven reliable from first principles. Given the wide range of differing approaches taken by the various groups developing simulators, this international code comparison effort is the first attempt to explore and understand the impacts of these modeling assumptions on production scenarios involving gas hydrates.

The intentions of the effort have been: (1) to exchange information regarding gas hydrate dissociation and physical properties enabling improvements in reservoir modeling, (2) to build confidence in all the leading simulators through exchange of ideas and cross-validation of simulator results on common datasets of escalating complexity, and (3) to establish a depository of gas hydrate related experiment/production scenarios with the associated predictions of these established

simulators that can be used for comparison purposes. Substantial progress toward these objectives has been realized and continues with long-term production models based on Alaskan North Slope data.

ACKNOWLEDGEMENTS

The authors would like to thank the U.S. Geological Survey, the Japan MH-21 project, and BP Exploration (Alaska) for supporting this effort. Portions of this technical effort were performed in support of the National Energy Technology Laboratory's on-going research in methane hydrates under the RDS contract DE-AC26-04NT41817.

REFERENCES

- [1] National Energy Technology Laboratory, http://www.netl.doe.gov/technologies/oil-gas/FutureSupply/MethaneHydrates/MH_CodeCompare/MH_CodeCompare.html. 2008.
- [2] Computer Modeling Group Ltd, *CMG STARS*. 2007: Calgary, Alberta, Canada.
- [3] Moridis, G.J., M.B. Kowalsky, and K. Pruess, *HydrateResSim Users Manual: A Numerical Simulator for Modeling the Behavior of Hydrates in Geologic Media*. Department of Energy, Contract No. DE-AC03-76SF00098. Lawrence Berkeley National Laboratory, Berkeley, CA, 2005.
- [4] MH-21 Research Consortium, <http://www.mh21japan.gr.jp/english/>.
- [5] White, M.D. and M. Oostrom., *STOMP Subsurface Transport Over Multiple Phase: User's Guide PNNL-15782 (UC-2010)*. Pacific Northwest National Laboratory, Richland, Washington, 2006.
- [6] Moridis, G.J., M.B. Kowalsky, and K. Pruess, *TOUGH-Fx/HYDRATE v1. 0 User's Manual: A code for the simulation of system behavior in hydrate-bearing geologic media*. Report LBNL-58950. Lawrence Berkeley National Laboratory, Berkeley, CA, 2005.
- [7] van Genuchten, M.T., *A closed-form equation for predicting the hydraulic conductivity of unsaturated soils*. Soil Sci. Soc. Am. J, 1980. **44**(5): p. 892-898.
- [8] Mualem, Y., *A New Model for Predicting the Hydraulic Conductivity of Unsaturated Porous Media*. 1976.
- [9] Stone, H.L., *Probability model for estimating three-phase relative permeability*. J. Pet. Tech, 1970. **22**(2): p. 214-218.
- [10] Aziz, K. and A. Settari, *Petroleum Reservoir Simulation*. 1979: Applied Science Publishers.
- [11] Anderson, B., et al. *Analysis of Modular Dynamic Formation Test Results from the "Mount Elbert" Stratigraphic Test Well, Milne Point, Alaska*. in *Proceedings of the 6th International Conference on Gas Hydrates*. 2008. Vancouver, British Columbia, Canada.